Published in final edited form as:
Nucl Med Biol. 2014 March ; 41(3): 282–289. doi:10.1016/j.nucmedbio.2013.12.002.

Gold nanorod-mediated hyperthermia enhances the efficacy of HPMA copolymer - ^{90}Y conjugates in treatment of prostate tumors

Brandon Buckway[1,2], **Nick Frazier**[2,3], **Adam J. Gormley**[2,3,#], **Abhijit Ray**[1,2], and **Hamidreza Ghandehari**[1,2,3,*]

[1]Department of Pharmaceutics and Pharmaceutical Chemistry, University of Utah, Salt Lake City, UT 84112, USA

[2]Center for Nanomedicine, Nano Institute of Utah, University of Utah, Salt Lake City, UT 84112, USA

[3]Department of Bioengineering, University of Utah, Salt Lake City, UT 84112, USA

Abstract

Introduction—The treatment of prostate cancer using a radiotherapeutic ^{90}Y labeled *N*-(2-hydroxypropyl)methacrylamide (HPMA)copolymer can be enhanced with localized tumor hyperthermia. An ^{111}In labeled HPMA copolymer system for single photon emission computerized tomography (SPECT) was developed to observe the biodistribution changes associated with hyperthermia. Efficacy studies were conducted in prostate tumor bearing mice using the ^{90}Y HPMA copolymer with hyperthermia.

Methods—HPMA copolymers containing 1, 4, 7, 10-tetraazacyclododecane-1,4,7,10-tetraacetic acid (DOTA) were synthesized by reversible addition-fragmentation transfer (RAFT) copolymerization and subsequently labeled with either ^{111}In for imaging or ^{90}Y for efficacy studies. Radiolabel stability was characterized in vitro with mouse serum. Imaging and efficacy studies were conducted in DU145 prostate tumor bearing mice. Imaging was performed using single photon emission computerized tomography (SPECT). Localized mild tumor hyperthermia was achieved by plasmonic photothermal therapy using gold nanorods.

Results—HPMA copolymer-DOTA conjugates demonstrated efficient labeling and stability for both radionuclides. Imaging analysis showed a marked increase of radiolabeled copolymer within the hyperthermia treated prostate tumors, with no significant accumulation in non-targeted tissues. The greatest reduction in tumor growth was observed in the hyperthermia treated tumors with ^{90}Y HPMA copolymer conjugates. Histological analysis confirmed treatment efficacy and safety.

Conclusion—HPMA copolymer-DOTA conjugates radiolabeled with both the imaging and treatment radioisotopes, when combined with hyperthermia can serve as an image guided approach for efficacious treatment of prostate tumors.

[*]Corresponding Author: Hamidreza Ghandehari, Ph.D., Departments of Pharmaceutics & Pharmaceutical Chemistry, and of Bioengineering, Utah Center for Nanomedicine, Nano Institute of Utah, University of Utah, 36 S Wasatch Dr, SMBB 5515, Salt Lake City, UT 84112, Phone: 801 587-1566, Fax: 801 581-6321, hamid.ghandehari@pharm.utah.edu.
Present address: Department of Materials, Imperial College London, London, SW7 2BP, United Kingdom.

Keywords

^{111}In; ^{90}Y; SPECT imaging; HPMA; hyperthermia; radiotherapy

Introduction

Prostate cancer is the most frequently diagnosed cancer in the U.S. [1]. Typically this disease affects men in their later years of life. With early screening the majority of patients can be appropriately treated with much success. However, it remains difficult to treat when the cancer is found in late or advanced stages. Treatment options typically start with surgical resection followed by hormone therapy, chemotherapy, biologic therapy or radiation therapy. Each of these treatments can cause distal or local adverse effects that can lead to lesser quality of life. Therefore, there remains a need to develop novel methods to treat prostate cancer that minimize the potential for side effects.

Macromolecular systems for delivery of therapeutics have been shown to passively target the tumor tissue via the enhanced permeability and retention (EPR) effect [2]. Leaky vasculature from angiogenesis due to the rapid tumor growth generates increased extravasation rates of macromolecules within the tumor region. Macromolecules do not easily diffuse from the normal vessels because the gaps in vascular walls are largely tight and intact. Evidence suggests that increased concentrations of these delivery systems containing therapeutics improve the treatment of cancer [3, 4].

The use of radionuclides for imaging and as radiotherapeutics has been shown to be effective in the diagnosis and treatment of many cancer types [5]. Yet, radiotherapeutics for cancer treatment have had limited application. This is in part due to insufficient localization and the non-specific uptake of radionuclides in the patient causing undesirable non-targeted tissue damage from radiation exposure. Several clinically approved radionuclides for therapy are conjugated to macromolecular tumor targeting monoclonal antibodies (MoAbs) in order to target only the specific diseased tissue [6]. However, tumor targets are heterogeneous in various patients and within individual tumors due to a variety of expression levels of the targeted antigen. One other shortfall of targeted delivery using MoAbs is that the target receptor is rarely only expressed on the targeted disease tissue which may lead to increased uptake in nonspecific tissues thereby increasing the chance of treatment related toxicity. There remains a need to target tumors using other macromolecular systems.

Use of water-soluble polymers based on *N*-(2-hydroxypropyl)methacrylamide (HPMA) is one potential method to increase radiotherapeutic accumulation in the tumor[7–9]. HPMA copolymers are ideal macromolecular carriers for radionuclide delivery because of their ability to be synthesized in a size controlled manner and presence of a variety of comonomers available to incorporate drugs, imaging agents or tumor targeting ligands [9–12]. Because of their macromolecular nature they are also able to passively target tumors via the enhanced permeability and retention (EPR) effect [2]. However, the delivery of HPMA copolymers and other macromolecules via the EPR effect has been variable from patient to patient [13]. Therefore, other methods must be considered to increase localization within the tumor.

Previous studies have shown the advantage of localized hyperthermia to increase HPMA copolymer conjugate localization and efficacy in treating prostate tumors [14–16]. Hyperthermia can be easily controlled and localized using plasmonic photothermal therapy (PPTT) [17]. PPTT uses the surface plasmon resonance of gold nanorods (GNR) when activated by the appropriate wavelength of light for controlled activation of heat [17].

Delivery of GNRs to the tumor is also based on passive accumulation and once localized to tumors can be irradiated by laser to augment the localization of subsequently injected polymer therapeutics [15].

The central hypothesis of this work is that by using localized hyperthermia with gold-nanorod-mediated plasmonic photothermal therapy, it is possible to enhance the delivery of HPMA copolymer-yttrium 90 conjugates to prostate tumors and improve radiotherapeutic efficacy. The overall design of the copolymer system described in this work includes side chain conjugated 1, 4, 7, 10-tetraazacyclododecane-1,4,7,10-tetraacetic acid (DOTA) for chelation of either ^{111}In for imaging of the biodistribution of the HPMA copolymers after hyperthermia treatment, or ^{90}Y for radiotherapeutic treatment of the tumor. ^{90}Y is a pure beta emitting isotope which is not an ideal imaging agent for γ-ray detection. Nuclear medicine techniques such as single photon emission computerized tomography (SPECT) offer relatively high resolution and quantitative images [18, 19]. Therefore imaging of HPMA copolymer ^{111}In using SPECT should provide more detailed information as to the quantity and kinetics of tumor localization and enable correlation of such localization with therapy. Correlation performed in this study between these two conjugates can give us a potential personalized therapy for use in treating prostate cancer.

Experimental Section

Materials and Methods

Chemicals—*N*-(3-Aminopropyl)methacrylamide hydrochloride (APMA) was acquired from Polysciences (Warrington, PA). 1, 4, 7, 10-tetraazacyclododecane-1,4,7,10-tetraacetic acid mono (*N*-hydroxysuccinimide ester) (DOTA-NHS-ester) was obtained from Macrocyclics (Dallas, TX). 2,2′-Azobis[2-(2-imidazolin-2-yl)propane] dihydrochloride (VA-044) was obtained from Wako Chemicals (Richmond, VA). [^{90}Y]YCl_3 and [^{111}In]$InCl_3$ was obtained from the Intermountain Radiopharmacy (Salt Lake City, UT). All other reagents were of reagent grade and were obtained from Sigma-Aldrich (St. Louis, MO).

Comonomer synthesis and characterization—*N*-(2-hydroxypropyl)methacrylamide comonomer (HPMA) was synthesized according to published methods [20]. 1, 4, 7, 10-tetraazacyclododecane-1,4,7,10-tetraacetic acid mono (*N*-(3-aminopropyl)methacrylamide (APMA-DOTA) was synthesized by combining a molar ratio of 1.5:1 DOTA-NHS-ester to APMA in anhydrous dimethylformamide (DMF) with 10% diisopropylethylamine (DIPEA) and stirred overnight at room temperature. The crude product was precipitated and excessively washed in diethyl ether to form a white powder. The final comonomer molecular weight (528.6 g/mol) was analyzed by electrospray ionization mass spectrometry (*m/z* calculated for $C_{23}H_{40}N_6O_8$, 528.5991, found 527 $[M-H]^+$, 549 $[M+Na]^+$).

Synthesis of the HPMA copolymer conjugate—HPMA and APMA-DOTA were copolymerized by reversible addition-fragmentation chain transfer (RAFT) polymerization according to Scheme 1. The radical initiator used was 2,2′-Azobis[2-(2-imidazolin-2-yl)propane]dihydrochloride (VA-044) and the chain transfer agent 2-cyano-2-propyl dodecyl trithiocarbonate (CPDT). At a molar ratio of 300:1:0.67 monomers/CPDT/VA-044 in methanol with total concentration of 1M, monomers were polymerized at 50°C for 24 hr in a nitrogen-purged sealed ampule to control the size and polydispersity of the HPMA copolymers. The final product was obtained by precipitating in diethyl ether and the resulting white solid was dissolved in deionized water and subsequently dialyzed using a 3.5 kDa molecular weight cut off (MWCO) dialysis bag (Spectrum Laboratories, Inc., Rancho Dominguez, CA). The purified copolymer was obtained by lyophilization and analyzed by Fast Protein Liquid Chromatography (FPLC) system (GE Healthcare, Piscataway, NJ)

equipped with a multi-angle light scattering (MALS) detector (Wyatt Technologies, Santa Barbara, CA). DOTA content was determined by analyzing gadolinium content (assuming a 1:1 ratio) after chelation according to previously described methods [21].

Radiolabeling with ^{111}In and ^{90}Y—HPMA copolymer-DOTA conjugate was labeled with radioisotopes according to previously published methods [22, 23]. 10 mg of HPMA copolymer-DOTA was dissolved in 250 μl of 1.0 M sodium acetate buffer pH 5.0. 10 mCi of [^{111}In]$InCl_3$ or [^{90}Y]YCl_3 was also treated with 0.25 ml of 1.0 M sodium acetate buffer pH 5.0. Radioactive compounds were added to the HPMA copolymer-DOTA solution and incubated at 50°C for 1.0 hr with mixing under nitrogen. The solution was allowed to cool to room temperature, and then treated with 100 μl of 0.05 M ethylenediaminetetraacetic acid (EDTA) for about 10 min in order to remove free or loosely bound $^{111}In^{+3}$ or $^{90}Y^{+3}$ ions. Radioactive polymers were purified by Sephadex G25 PD-10 columns (GE Life Sciences, Piscataway, NJ). Radioactivity was measured using a CAPTUS 3000 multichannel analyzer (Canberra Industries, Inc., Meriden, CT). Radiostability was determined by incubating radiolabeled copolymers at 37°C in the presence of mouse serum. Samples were collected at 24, 48 and 72 hr and subjected to PD-10 column separation to determine the free radiolabel content.

Synthesis of PEGylated gold nanorods—Gold nanorods (GNRs) were synthesized using the seed-mediated growth method with an aspect ratio that correlates to a surface plasmon resonance (SPR) peak between 800 and 810 nm [24]. The light absorption profile was measured by UV spectrometry. The GNRs were then centrifuged and washed three times with deionized water to remove excess hexadecyltrimethylammonium bromide (CTAB). After washing, poly(ethylene glycol) (PEG) (methoxy-PEG-thiol 5 kD, Creative PEGWorks, Winston Salem, NC) was added to the GNR suspension and stirred for 1 h to allow for sufficient coating. The PEG-GNRs were then dialyzed (10k MWCO, Spectrum labs), centrifuged, washed, and concentrated to remove any excess, unbound PEG. The final concentration of the PEG-GNRs was 1.2 mg/ml (OD = 120) and were stored at 4°C. Finally, the PEG-GNR solution was sterile filtered prior to use *in vivo.*

Animal tumor model—DU-145 prostate tumor cells (ATCC, Manassas, VA) were cultured in Eagle's Minimum Essential Medium (EMEM) (ATCC, Manassas, VA) supplemented with 10% (v/v) fetal bovine serum (FBS) at 37°C in a humidified atmosphere of 5% CO_2 (v/v). Cell cultures were harvested at approximately 80% confluence by treatment with TrypLE™ Express (Invitrogen, Grand Island, NY) and subsequent dilution in phosphate buffered saline (PBS). Athymic Nu/Nu female mice were inoculated with 1×10^7 cells on both the left and right lower flanks of each mouse. Experiments were initiated after tumor diameters had reached 5 7 mm in diameter by external caliper measurement. All animal experiments were conducted under an approved protocol from the Institutional Animal Care and Use Committee at the University of Utah (Salt Lake City, UT).

Biodistribution of ^{111}In HPMA copolymer-DOTA conjugates—The general method of plasmonic photothermal therapy for moderate hyperthermia is demonstrated in Figure 1. Prostate tumor bearing mice were administered 9.6 mg/kg of PEGylated GNRs via lateral tail vein injection and allowed to passively accumulate in the tumor via the EPR effect for 48 hr. After 48 hr mice were injected with 300–350 μCi of ^{111}In labeled HPMA copolymer-DOTA conjugates and immediately treated on the right tumor with moderate hyperthermia as described previously [15]. Briefly, the right tumor of the mouse was irradiated by laser at a wavelength of 808 nm for 10 minutes. Temperature was measured using a needle point temperature probe near the center of the tumor and laser power was adjusted in order to maintain tumor temperature at 43±1°C. The mouse was anesthetized by isofluorane via nose

cone and immediately placed on the bed of an Inveon microPET/SPECT/CT multimodality scanner (Siemens Medical Solutions USA, Inc., Malvern, PA) and imaged by single photon emission computerized tomography (SPECT) for 4 hrs. SPECT scans were performed in 22 min frames with an x-ray computerized tomography (CT) scan performed at the beginning and end of the 4 hr SPECT series. A follow up static SPECT/CT scan was also conducted at 24 hrs the following day. After 24 hrs, the mouse was euthanized and organs collected (blood, heart, lung, liver, spleen, kidney and tumors). The organs were weighed and gamma counted using a CAPTUS 3000 well counter. SPECT images were analyzed using the Inveon Research Workplace software (Siemens Medical Solutions USA, Inc., Malvern, PA) with regions of interest (ROI) drawn respective to the tumors shown on the CT image with SPECT registration. The estimated average voxel intensity obtained from each ROI of each tumor was correlated to the gamma counted tissues excised at the 24 hr time point of each mouse. Left and right tumors were compared to determine differences in pharmacokinetic and biodistribution profiles from the imaging and necropsy data related to the hyperthermia treatment using GraphPad Prism Software (La Jolla, CA). The area under the curve (AUC) was determined using the trapezoid method via the same software.

Combination radiotherapy and hyperthermia treatment—Prostate tumor animal models treated with PEGylated GNRs were prepared as described above and injected with 250 μCi of ^{90}Y labeled HPMA copolymer-DOTA conjugates via the lateral tail vein injection. The right tumor of the mouse was subjected to moderate hyperthermia as described above. A saline (hyperthermia only) control group was also treated in a similar manner. Left and right tumor ellipsoid volumes were estimated by external caliper measurement of the length and width of each tumor twice weekly. Tumor volumes were normalized to measurement on day 0 of treatment. Animal tumor weights were monitored. At the end of the 40 day study the mice were euthanized and heart, lung, liver, spleen, kidney and both tumors were collected and incubated in 10% neutral buffered formalin for 48 hrs. The tissues were subsequently sliced into 5 μm slices and hematoxylin and eosin (H&E) stained by the Histology Department at ARUP Laboratories (Salt Lake City, UT). Tissue slides were analyzed for toxicity related to radioactive exposure from the ^{90}Y HPMA copolymer-DOTA conjugate treatment. Tumor tissues were also investigated for evidence of radiotherapeutic damage.

Statistical analysis—Animal study results were analyzed for statistical significance using one-way ANOVA with Tukey's post-test and biodistribution results between tumor treatments were analyzed by the student T-test using GraphPad Prism Software (La Jolla, CA).

Results and Discussion

The overall goal for this study was to evaluate a polymer containing both an imaging agent and a radiotherapeutic in conjunction with localized hyperthermia. The polymer was designed to reduce non-specific uptake, allow urinary clearance and assure sufficient uptake within the tumor mass. Characteristics of the copolymers are shown in Table 1. A polymer of less than 45 kDa was desired in order to minimize the lifetime of the HPMA copolymer in the body [2]. The DOTA content was expected to be 10 wt% based on the feed content of the copolymer (2.0 mol%). DOTA content was sufficient for ^{111}In and ^{90}Y radiolabelling demonstrated by the radioactive content shown in Table 1.

DOTA has been shown to be a stable chelator for both radioisotopes [22, 25]. ^{111}In is a common γ-emitting radionuclide used in the clinic for SPECT imaging [26]. ^{90}Y as a beta emitting radionuclide has been clinically used for radiotherapeutic treatment of tumors [27]. ^{111}In and ^{90}Y have similar half-lives (2.80 and 2.67 days, respectively) that correspond

to the potential biological half-life of HPMA copolymer construct. This allowed sufficient monitoring by imaging and radioactivity exposure for treatment of the tumor. The imaging construct based on ^{111}In allowed image-based biodistribution and pharmacokinetic profiles that can predict therapeutic safety and efficacy of the ^{90}Y radiotherapeutic construct. Stability of the ^{90}Y with HPMA copolymer-DOTA conjugate in the presence of serum is shown in Figure 2. The ^{90}Y labeled conjugate was ~93% stable over 72 hrs in mouse serum after separation on the PD-10 column. This could be caused by radiolysis of some of the label due to the high beta energy of ^{90}Y and lack of any scavenger in the formulation.

The results from the animal imaging study of the ^{111}In labeled HPMA copolymer-DOTA conjugate demonstrate increased localization in the tumor with moderate hyperthermia. Figure 3A–C demonstrates that hyperthermia treated tumors (right tumor) have a marked increased localization of the HPMA copolymer over time. It also demonstrates that the most off-target overall exposure in the animal is likely the kidneys. Based on the ^{111}In imaging version of the HPMA copolymer, the right tumor received a higher average exposure of beta particle emission than that of the left tumor due to hyperthermia treatment. Time activity concentration curves determined from image analysis was performed for each tumor (hyperthermia treated and control). Average voxel intensity from SPECT/CT images were calibrated based on the necropsied tissue counts of both tumors of each mouse collected at the 24 h time point (n = 3) (Figure 3E). Radioactivity exposure to the tumor was measured by calculating the AUC for 0–4 h and 4–24 h using the trapezoidal method. The hyperthermia treated tumor $AUC_{0–4\ hr}$ = 1990 ± 310 %ID·min/g and $AUC_{4–24\ hr}$ = 9107 ± 1512 %ID·min/g. The control tumors $AUC_{0–4\ hr}$ = 648.5 ± 62.4 %ID·min/g and $AUC_{4–24\ hr}$ = 2994 ± 391 %ID·min/g. The amount of exposure is about 3 times higher for the hyperthermia treated animals during both periods of 0–4 and 4–24 h. The accuracy during elimination phase (4–24 h) is limited based on the lack of data points between 4–24 h. However, the AUC ratios between both regions of the time activity curve are very similar ($AUC_{0–4\ hr}$ ratio = 3.07 and $AUC_{4–24\ hr}$ = 3.04) suggesting that the elimination phase fit is relatively accurate as we should expect the ratio of exposure to the tumors to be the same. SPECT imaging is known to have limitations in absolute quantitation and is normally considered semi-quantitative due to a lack of ability to correct for scattering, attenuation and other related factors that can skew imaging results. The data from this imaging study compares the left and right tumors of the same animal and can therefore represent a fairly accurate comparison. Overall, the imaging data analysis clearly demonstrates an increased accumulation of the radiolabeled polymer. This overall increase in exposure to the hyperthermia treated tumor can be related to the beta emitting ^{90}Y radiolabeled HPMA construct and effectively explain the efficacy results discussed below.

The efficacy study shows the clear advantage of using moderate hyperthermia to improve the delivery and efficacy of ^{90}Y radiotherapy (Figure 4). Radiotherapy was only effective in the tumor treated with hyperthermia. This is expected due to the fact that we see more of the radiolabeled copolymers localizing in the tumor over time. Hyperthermia increases blood flow and perfusion to the tumor [28, 29], thus potentially augmenting the EPR effect and localization of HPMA copolymers. It is also possible that the increased perfusion to the tumor region may sensitize the tumor to the effects of radiation. This can be due to the increased oxygenation of the tumor delivered from the increased blood flow. Hyperthermia alone to the tumors using PPTT also had a significant effect but to a lesser extent. This is similar to results conducted in a similar study performed previously [16]. Despite the mild temperature increase in the overall tumor measured by the needle thermal couple, the local temperature near the gold nanorods may be higher and cause some vascular damage and disruption. This may lead to temporary starvation of the tumor that demonstrates reduced tumor growth and could explain the efficacy related to hyperthermia alone. Interestingly, the radiotherapy alone had no efficacy in this study. This can be explained based on the fact that

the biodistribution studies in Figure 4 show much less accumulation of the radioactivity in the tumors. The fact that hyperthermia has the potential to sensitize tumors to radiotherapy, also is supported based on these results.

The normalized animal weights shown in Figure 5 demonstrate that the treatment was well tolerated. Histological analysis displayed in Figure 6 also demonstrates the lack of damage to the primary organs of the mice. From the biodistribution studies the normal tissue/organ most exposed to radiation was the kidneys (Figure 3). A time activity curve of the overall kidney exposure and relevant discussion can be found in the supplemental data section. However, kidney samples showed a normal structure of both glomerulus and proximal tubule regions thus demonstrating resistance to irreversible beta-emission related damage. Possible evidence of radiation damage to the tumor is demonstrated in Figure 6 due to increased fibrosis, vacuolization and increased number of apoptotic bodies. These effects are similar to results found in previous studies using ^{90}Y radiotherapy [30, 31]. Further analysis was performed by comparing the differences in the amounts of necrotic tissue in the treated tumors versus non-treated tumors shown in Figure 7. Some of the necrotic tissue is a result of rapid tumor growth in this animal model. Therefore, areas of necrosis from treatment were measured using image analysis software and compared to control mice. Necrosis in the combination radiotherapy and hyperthermia treated group was found to be approximately 5 times greater than that of control. This increase in levels of tissue damage is a result of the treatment and explains effects observed in the efficacy results (Figure 2.)

This study demonstrates the enhanced efficacy to prostate cancer treatment with ^{90}Y HPMA copolymers in combination with gold nanorod mediated hyperthermia. One of the advantages of this system compared to other macromolecular radiotherapeutics that have been developed is the increased localization by external trigger and without increasing non-targeted tissue uptake. Targeting of the tumor for both the GNRs and the HPMA copolymers is via the EPR effect. One of the detriments to the EPR effect is the lack of sufficient quantities accumulating in the tumor of therapeutics. This particular approach not only increases the EPR effect presumably due to increased permeation and blood flow to the tumor but also sensitizes the tumor to the therapeutic. The intervention of laser irradiation assures that the effect is targeted to only the tumor region and thus improves the targeted delivery only within the desired location.

The size of HPMA copolymers used in this study were designed to eventually eliminate from the body but have sufficient circulation time to distribute into the hyperthermia treated tumors. However, the EPR effect of HPMA copolymers and other macromolecules has been shown to be enhanced by using larger molecular weight carriers based on longer circulation times due to their inability to be filtered through the pores in the glomerulus of the kidney. This may be detrimental because the longer the conjugates remain in the body the more likely the radiolabel can be released and distributed to undesirable organs and cause toxicity. However, recent large degradable HPMA copolymers have shown eventual clearance due to enzymatically cleavable spacers in the backbone of the polymer construct [32]. These conjugates showed a marked increase in tumor localization compared to small molecular weight systems and suggest that radiotherapeutic delivery could also be enhanced using this method.

One emerging method for administering controlled localized hyperthermia is high intensity focused ultrasound (HIFU) [33]. This method could potentially have a similar effect in enhancing the delivery of polymer therapeutics. Although gold nanoparticles have shown no acute toxic effects, it has yet to be determined if the long-term exposure from the non-eliminated GNRs in the body may cause toxicity. Also the penetration of light to activate the hyperthermia response with GNRs is limited in tissue depth. HIFU is widely available for

clinical use and in combination with radiotherapy using HPMA copolymer delivery may accelerate the development of externally targeted approaches such as the one described in this study.

The radionuclides used in this study for HPMA copolymer delivery of radiotherapeutics are similar to those used in the clinic for image guided therapy. Bexxar® and Zevalin® are monoclonal antibodies used in the delivery of both radioisotopes for imaging and therapy [6]. Imaging of these therapies using SPECT is utilized to predict safety of the subsequently administered radiotherapeutic version. The HPMA copolymer system developed in this study could be used in a similar way for prostate cancer. The imaging version could be used to visualize any non-specific uptake that may exist in a particular patient and could also be used to measure the amount localized in the tumor. The ^{111}In labeled HPMA copolymer imaging version provides information about the quantity localized in the prostate tumor. This quantitation is useful in determining the dose required for efficacy of the ^{90}Y labeled HPMA copolymers used for radiotherapy. This strategy can potentially provide the prostate cancer patient with a personalized therapy that increases the efficiency, safety and efficacy of anti-cancer treatment.

Conclusion

The HPMA copolymers radiolabeled with ^{90}Y for combination radiotherapy and hyperthermia were found to be effective in treatment of prostate tumors in a mouse model. HPMA copolymers were successfully monitored by SPECT imaging for biodistribution effects related to hyperthermia. The radioactive treatment was found to be primarily accumulated in the tumor. Histological examination of the various organs did not show evidence of any radioactive related toxicity. Overall, the conjugates were proven to be a potentially safe and efficacious treatment for prostate cancer.

Supplementary Material

Refer to Web version on PubMed Central for supplementary material.

Acknowledgments

The authors would like to thank the Small Animal Imaging Core Lab at the University of Utah for their assistance in performing the SPECT/CT imaging and analysis in these experiments. We would also like to thank Dr. Lawrence McGill of ARUP Laboratories for his assistance in examining the histology results.

References

1. American Cancer Society. Cancer Facts and Figures 2012. Atlanta, GA: American Cancer Society; 2012.
2. Noguchi Y, Wu J, Duncan R, Strohalm J, Ulbrich K, Akaike T, et al. Early phase tumor accumulation of macromolecules: a great difference in clearance rate between tumor and normal tissues. Jpn J Cancer Res. 1998; 89:307–14. [PubMed: 9600125]
3. Maeda H, Bharate GY, Daruwalla J. Polymeric drugs for efficient tumor-targeted drug delivery based on EPR-effect. Eur J Pharm Biopharm. 2009; 71:409–19. [PubMed: 19070661]
4. Maeda H, Sawa T, Konno T. Mechanism of tumor-targeted delivery of macromolecular drugs, including the EPR effect in solid tumor and clinical overview of the prototype polymeric drug SMANCS. J Control Release. 2001; 74:47–61. [PubMed: 11489482]
5. Kramer-Marek G, Capala J. The role of nuclear medicine in modern therapy of cancer. Tumour Biol. 2012; 33:629–40. [PubMed: 22446937]
6. Goldsmith SJ. Radioimmunotherapy of lymphoma: Bexxar and Zevalin. Semin Nucl Med. 2010; 40:122–35. [PubMed: 20113680]

7. Kopecek J. Polymer-drug conjugates: origins, progress to date and future directions. Adv Drug Deliv Rev. 2013; 65:49–59. [PubMed: 23123294]
8. Kopecek J, Kopeckova P, Minko T, Lu Z. HPMA copolymer-anticancer drug conjugates: design, activity, and mechanism of action. Eur J Pharm Biopharm. 2000; 50:61–81. [PubMed: 10840193]
9. Lu ZR. Molecular imaging of HPMA copolymers: visualizing drug delivery in cell, mouse and man. Adv Drug Deliv Rev. 2010; 62:246–57. [PubMed: 20060431]
10. Kopecek J, Kopeckova P. HPMA copolymers: origins, early developments, present, and future. Adv Drug Deliv Rev. 2010; 62:122–49. [PubMed: 19919846]
11. Mitra A, Nan A, Line BR, Ghandehari H. Nanocarriers for nuclear imaging and radiotherapy of cancer. Curr Pharm Des. 2006; 12:4729–49. [PubMed: 17168775]
12. Pike DB, Ghandehari H. HPMA copolymer-cyclic RGD conjugates for tumor targeting. Adv Drug Deliv Rev. 2010; 62:167–83. [PubMed: 19951733]
13. Lammers T, Kiessling F, Hennink WE, Storm G. Drug targeting to tumors: principles, pitfalls and (pre-) clinical progress. J Control Release. 2012; 161:175–87. [PubMed: 21945285]
14. Gormley AJ, Larson N, Banisadr A, Robinson R, Frazier N, Ray A, et al. Plasmonic photothermal therapy increases the tumor mass penetration of HPMA copolymers. J Control Release. 2013; 166:130–8. [PubMed: 23262203]
15. Gormley AJ, Larson N, Sadekar S, Robinson R, Ray A, Ghandehari H. Guided delivery of polymer therapeutics using plasmonic photothermal therapy. Nano today. 2012; 7:158–67. [PubMed: 22737178]
16. Larson N, Gormley AJ, Frazier N, Ghandehari H. Synergistic enhancement of cancer therapy using a combination of heat shock protein targeted HPMA copolymer-drug conjugates and gold nanorod induced hyperthermia. J Control Release. 2013; 170:41–50. [PubMed: 23602864]
17. Huang X, Jain PK, El-Sayed IH, El-Sayed MA. Plasmonic photothermal therapy (PPTT) using gold nanoparticles. Laser M ed Sci. 2008; 23:217–28.
18. Alberini JL, Edeline V, Giraudet AL, Champion L, Paulmier B, Madar O, et al. Single photon emission tomography/computed tomography (SPET/CT) and positron emission tomography/computed tomography (PET/CT) to image cancer. J Surg Oncol. 2011; 103:602–6. [PubMed: 21480254]
19. Weissleder, R. Molecular imaging: principles and practice. Shelton, CT: People's Medical Pub. House-USA; 2010.
20. Strohalm J, Kopecek J. Poly N-(2-hydroxypropyl) methacrylamide: 4. Heterogenous polymerization. Angew Makromol Chem. 1978; 70:109–18.
21. Zarabi B, Borgman MP, Zhuo J, Gullapalli R, Ghandehari H. Noninvasive monitoring of HPMA copolymer-RGDfK conjugates by magnetic resonance imaging. Pharm Res. 2009; 26:1121–9. [PubMed: 19160028]
22. Kukis DL, DeNardo SJ, DeNardo GL, O'Donnell RT, Meares CF. Optimized conditions for chelation of yttrium-90-DOTA immunoconjugates. J Nucl Med. 1998; 39:2105–10. [PubMed: 9867151]
23. Mitra A, Nan A, Papadimitriou JC, Ghandehari H, Line BR. Polymer-peptide conjugates for angiogenesis targeted tumor radiotherapy. Nucl Med Biol. 2006; 33:43–52. [PubMed: 16459258]
24. Nikoobakht B, Burda C, Braun M, Hun M, El-Sayed MA. The quenching of CdSe quantum dots photoluminescence by gold nanoparticles in solution. Photochem Photobiol. 2002; 75:591–7. [PubMed: 12081320]
25. Liu S, Pietryka J, Ellars CE, Edwards DS. Comparison of yttrium and indium complexes of DOTA-BA and DOTA-MBA: models for (90)Y- and (111)In-labeled DOTA-biomolecule conjugates. Bioconjug Chem. 2002; 13:902–13. [PubMed: 12121149]
26. Biersack, HJ. Clinical nuclear medicine. Berlin; New York: Springer; 2007.
27. Goffredo V, Paradiso A, Ranieri G, Gadaleta CD. Yttrium-90 (90Y) in the principal radionuclide therapies: an efficacy correlation between peptide receptor radionuclide therapy, radioimmunotherapy and transarterial radioembolization therapy. Ten years of experience (1999–2009). Crit Rev Oncol Hematol. 2011; 80:393–410. [PubMed: 21388824]
28. Griffin RJ, Dings RP, Jamshidi-Parsian A, Song CW. Mild temperature hyperthermia and radiation therapy: role of tumour vascular thermotolerance and relevant physiological factors. International

Journal of Hyperthermia: the Official Journal of European Society for Hyperthermic Oncology, North American Hyperthermia Group. 2010; 26:256–63.

29. Song CW, Park HJ, Lee CK, Griffin R. Implications of increased tumor blood flow and oxygenation caused by mild temperature hyperthermia in tumor treatment. International Journal of Hyperthermia: the Official Journal of European Society for Hyperthermic Oncology, North American Hyperthermia Group. 2005; 21:761–7.
30. Huang J, Chunta JL, Amin M, Lee DY, Grills IS, Wong CY, et al. Detailed characterization of the early response of head-neck cancer xenografts to irradiation using (18)F-FDG-PET imaging. Int J Radiat Oncol Biol Phys. 2012; 84:485–91. [PubMed: 22331000]
31. Stone HB, Coleman CN, Anscher MS, McBride WH. Effects of radiation on normal tissue: consequences and mechanisms. Lancet Oncol. 2003; 4:529–36. [PubMed: 12965273]
32. Zhang R, Luo K, Yang J, Sima M, Sun Y, Janat-Amsbury MM, et al. Synthesis and evaluation of a backbone biodegradable multiblock HPMA copolymer nanocarrier for the systemic delivery of paclitaxel. J Control Release. 2013; 166:66–74. [PubMed: 23262201]
33. Sanches PG, Grull H, Steinbach OC. See, reach, treat: ultrasound-triggered image-guided drug delivery. Ther Deliv. 2011; 2:919–34. [PubMed: 22833903]

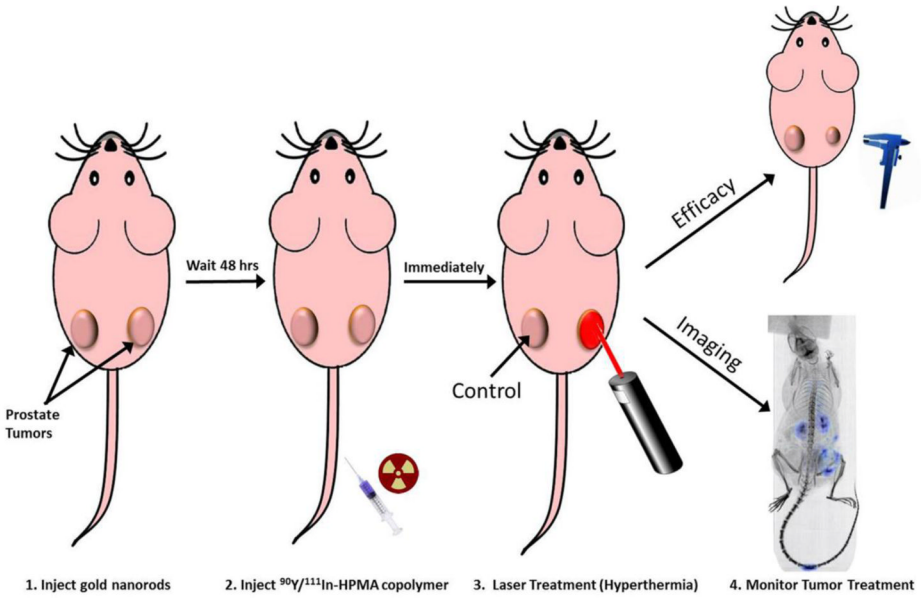

Figure 1.
Methodology for combination radiotherapy and hyperthermia treatment in prostate tumor bearing mice.

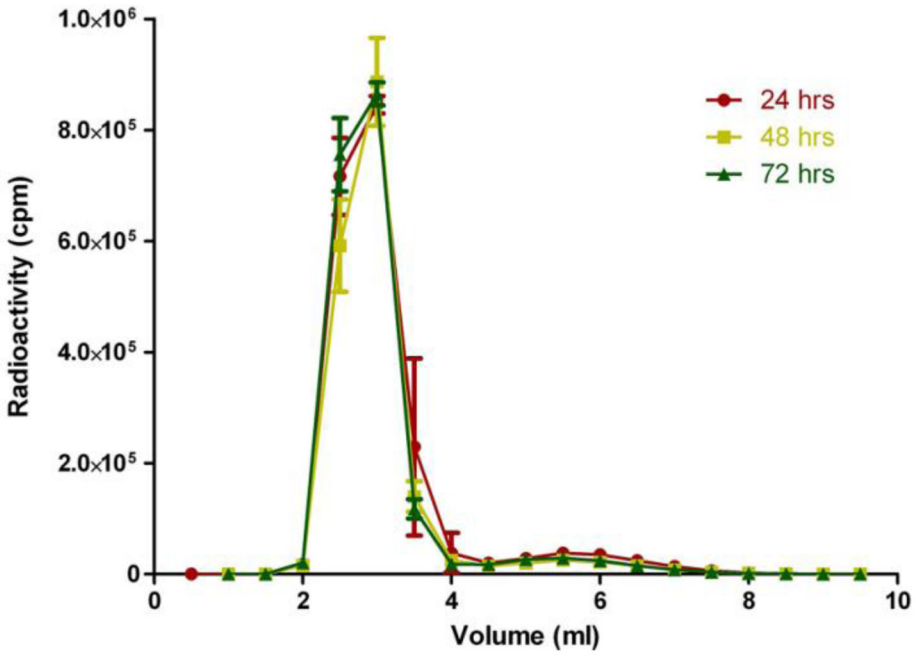

Figure 2. Radiostability of the ^{90}Y labeled HPMA copolymer-DOTA

Data is represented as the mean ± standard error of the mean (SEM) (n=3). An average amount of approximately 93% was observed as macromolecular in size corresponding to the radiolabeled HPMA copolymer.

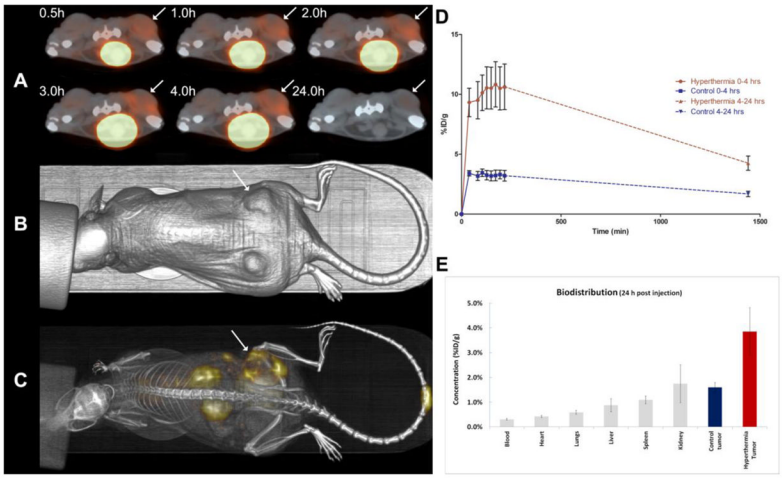

Figure 3. Biodistribution and pharmacokinetic analysis of ^{111}In labeled HPMA copolymer-DOTA

A) Serial 22 min axial scans showing a comparison of the right (hyperthermia treated) and left tumors on the dorsal region of the animal injected 300 μCi of ^{111}In-HPMA copolymer while under isofluorane. The large bright spot central to the anterior side of the animal is a result of a large accumulation in the bladder demonstrating the eventual clearance of the HPMA copolymer conjugates. Arrows denote hyperthermia treated tumor. B) CT image of the mouse showing the lower dorsal placement of the tumors. C) Whole body planar image at approximately 4 h post-injection. D) Biodistribution and pharmacokinetic analysis of ^{111}In labeled HPMA copolymer-DOTA. Time activity graph showing the curve fits for the calculations of AUC for each tumor. Red line represents the right (hyperthermia) tumor and the blue line represents the left (control) tumor. Data represented as the mean ± SEM (n=3). The hyperthermia treated tumor $AUC_{0–4\ hr}$ = 1990 %ID·min/g and $AUC_{4–24\ hr}$ = 9107 %ID·min/g. The control tumors $AUC_{0–4\ hr}$ = 648.5 %ID·min/g and $AUC_{4–24\ hr}$ = 2994 %ID·min/g. The dashed lines represent the elimination phases in which the accuracy is limited based on limited data points for analysis. E) The biodistribution data from the γ-counting of each individual organ at 24 h post injection. Data represented as the mean ± SEM (n=3).

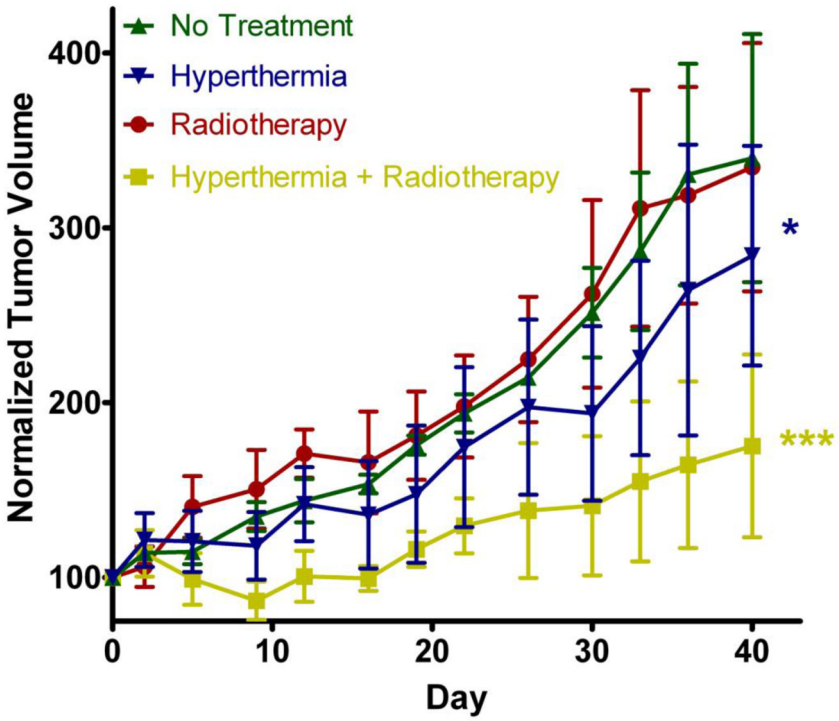

Figure 4. Efficacy of ^{90}Y HPMA copolymer-DOTA conjugates

Efficacy data for 40 days treatment comparing radiotherapy and hyperthermia combinations. No Treatment (Green) and hyperthermia (Blue) data are represented as mean ± SEM (n=3). Radiotherapy (Red) and hyperthermia + radiotherapy (Yellow) are represented as mean ± SEM (n=5). Statistical significance was analyzed by repeated measure ANOVA using Tukey's post-test with hyperthermia (Blue) group (*) statistically different ($p < 0.01$) than control and radiotherapy alone. The combination hyperthermia + radiotherapy (yellow) group (***) was also found to be statistically different ($p < 0.0001$) than all other groups.

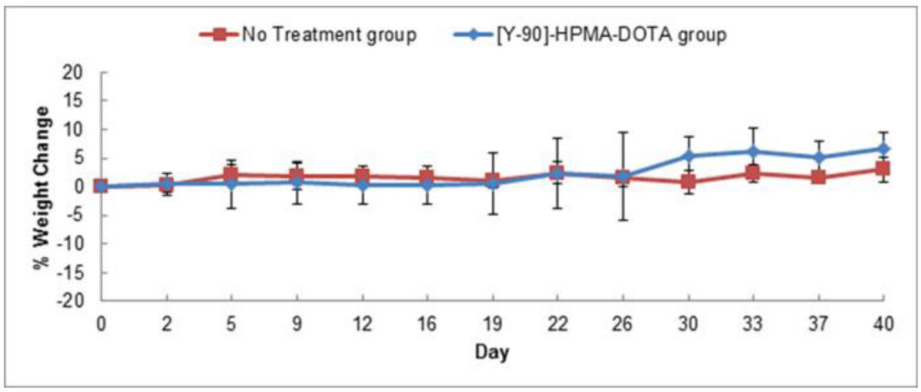

Figure 5. Normalized animal weight change

No treatment effect related to weight-loss was observed on either group of animals. No treatment group includes both no treatment and hyperthermia alone groups and the [Y-90]-HPMA-DOTA group includes both radiotherapy alone and combination groups from Figure 4.

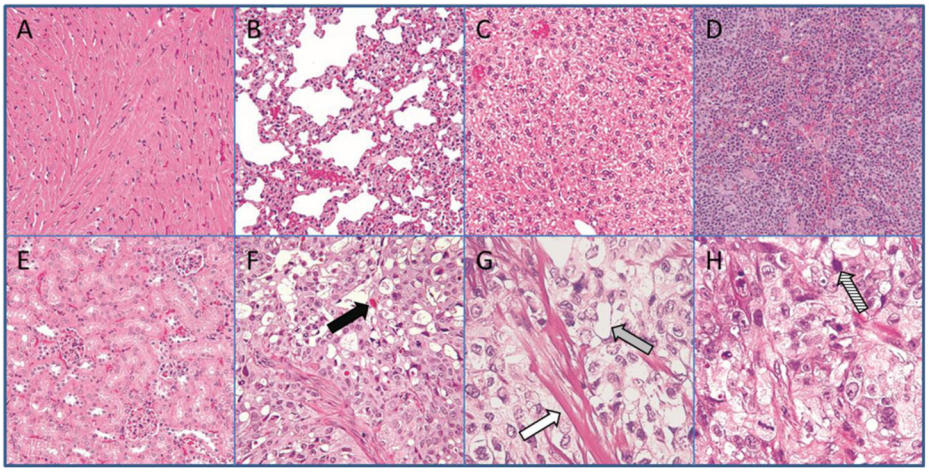

Figure 6. Histology

Representative samples removed at the end of the 40 day study and stained using H&E staining. Organs showed no difference compared to controls. Arrows represent potential types of evidence for radiation related effects from ^{90}Y-HPMA copolymer-DOTA and hyperthermia treatment.

A) Heart (magnification 40×)
B) Lung (40×)
C) Liver (40×)
D) Spleen (40×)
E) Kidney (40×)
F) Radiotherapy treated tumor (40×)
G) Radiotherapy treated tumor (100×)
H) Radiotherapy treated tumor (100×)
Solid black arrow = thanatosome infiltration
White arrow = Fibrosis
Grey arrow = Vacuole formation
Striped arrow = Apoptotic bodies

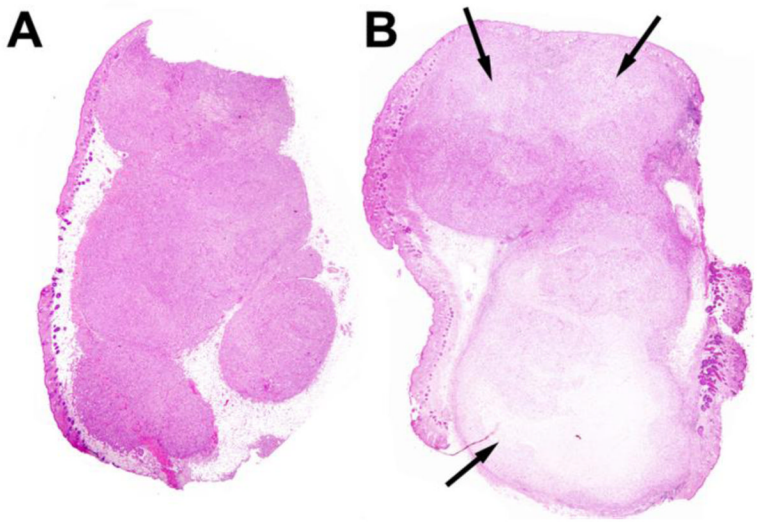

Figure 7. Histological comparison of necrosis

H&E stained tumor slices representative of: A) normal mouse tumor and B) radiotherapy + hyperthermia treated tumor. Arrows represent areas of necrosis.

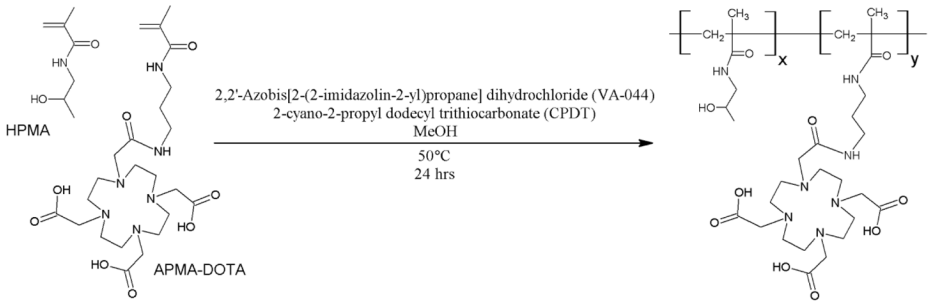

Scheme 1.
RAFT polymerization of HPMA-DOTA

Table 1

HPMA copolymer-DOTA characteristics

Polymer Characteristics	Result
$\mathbf{M_w}^a$	27.7 kDa
$\mathbf{M_n}^a$	25.5 kDa
PDI[a]	1.09
APMA-DOTA feed ratio	2.0 mol%
^{111}In content[b]	571 μCi/mg
^{90}Y content[b]	356 μCi/mg

[a] Determined by MALS

[b] Determined by γ-counter at end of synthesis